Supplementary materials for the manuscript "Lidar observations of cirrus cloud properties with CALIPSO from midlatitudes towards high latitudes"

Qiang Li and Silke Groß

Deutsches Zentrum für Luft- und Raumfahrt, Institut für Physik der Atmosphäre, D-82234 Oberpfaffenhofen, Germany,

Correspondence: Qiang Li (qiang.li@dlr.de)

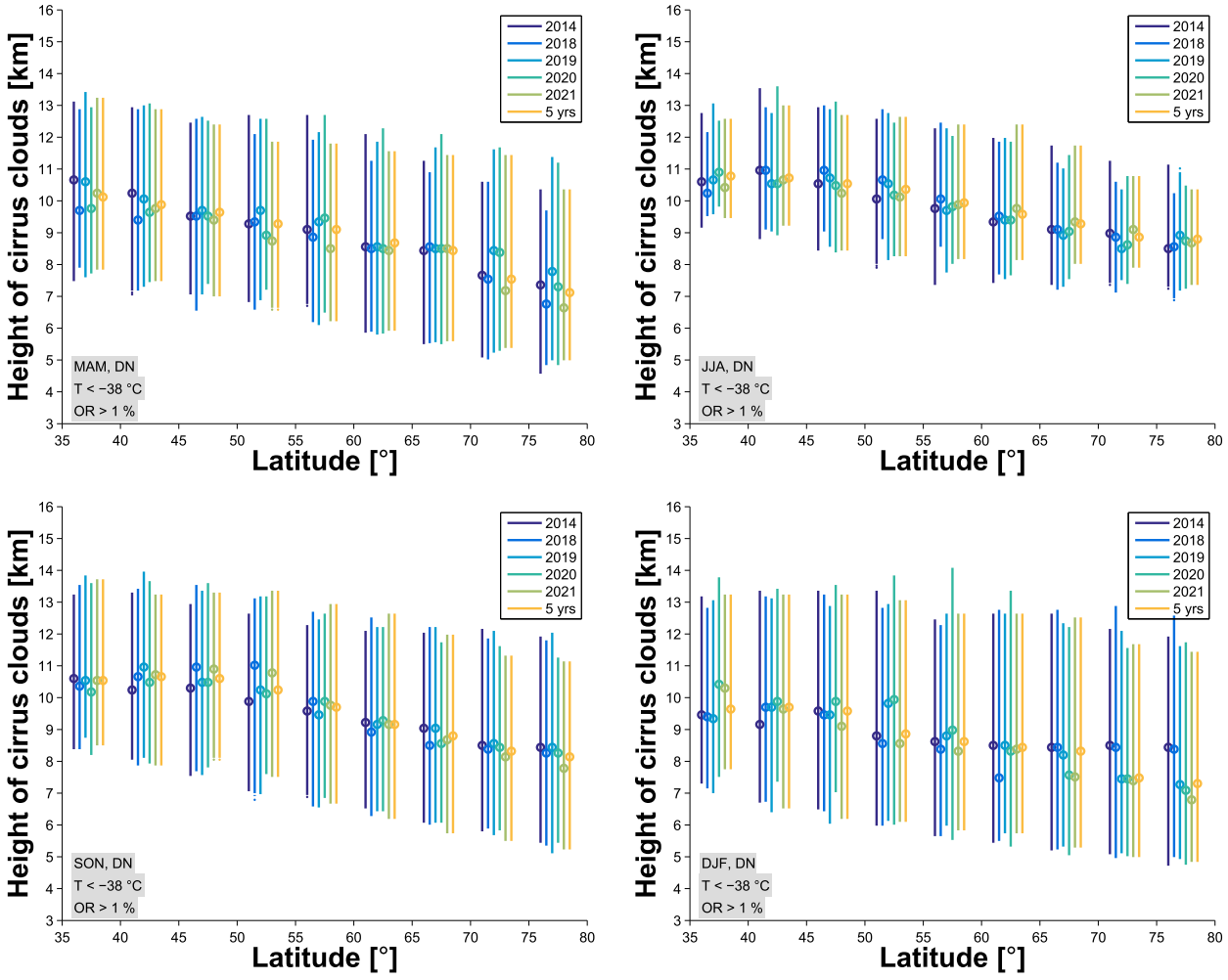

Figure S1. Altitude ranges of cirrus cloud formation restricted with the occurrence rate > 1% alongside the altitudes with the maximum occurrence rate indicated with circles in different years (2014 and 2018-2021) and the composite mean values from all the 5-year observations. The panels from left to right and from upper to lower show the results in different seasons, respectively.

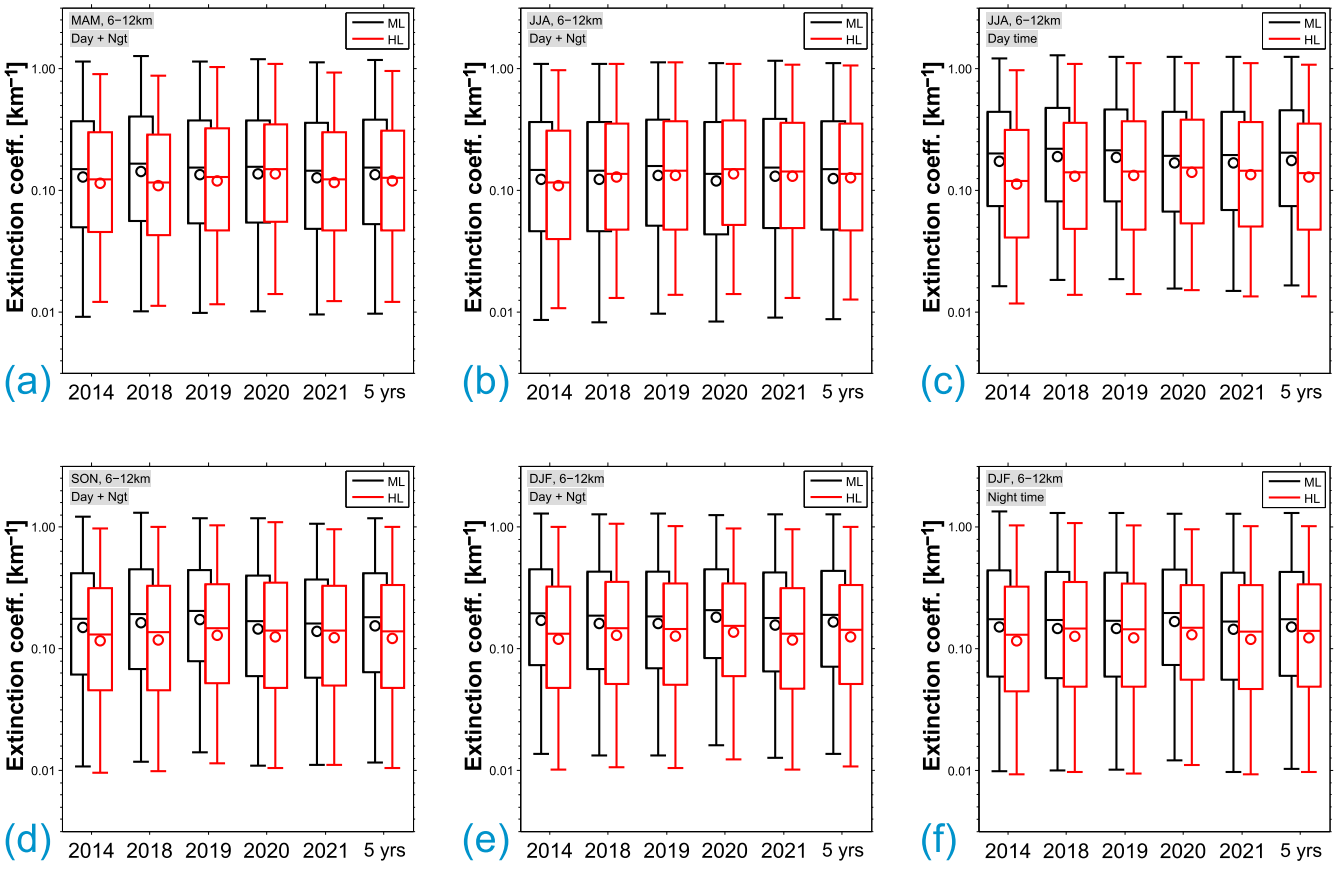

Figure S2. Box plot representations of the extinction coefficients of ice crystals within cirrus clouds observed with CALIPSO in different seasons in years of 2014 and 2018–2021 as well as the composite results in the 5 years (in panels a, b, e, and f). The results in the high-latitude regions are shown in red and midlatitude in black. Boxes represent the 25th–75th percentiles (top and bottom). Solid lines through the corresponding boxes stand for the medians and circles for means. Whiskers indicate the 5th and 95th percentiles, and outliers with values falling within the largest 5% and smallest 5% of the distributions of extinction coefficients are not shown here. Considering the occurrence of polar day and polar night in summer and winter, respectively, we also indicate the results only from the day-time measurements in the summer months and from the night-time measurements in the winter months for a fair comparison in different latitudes (in panels c and g).

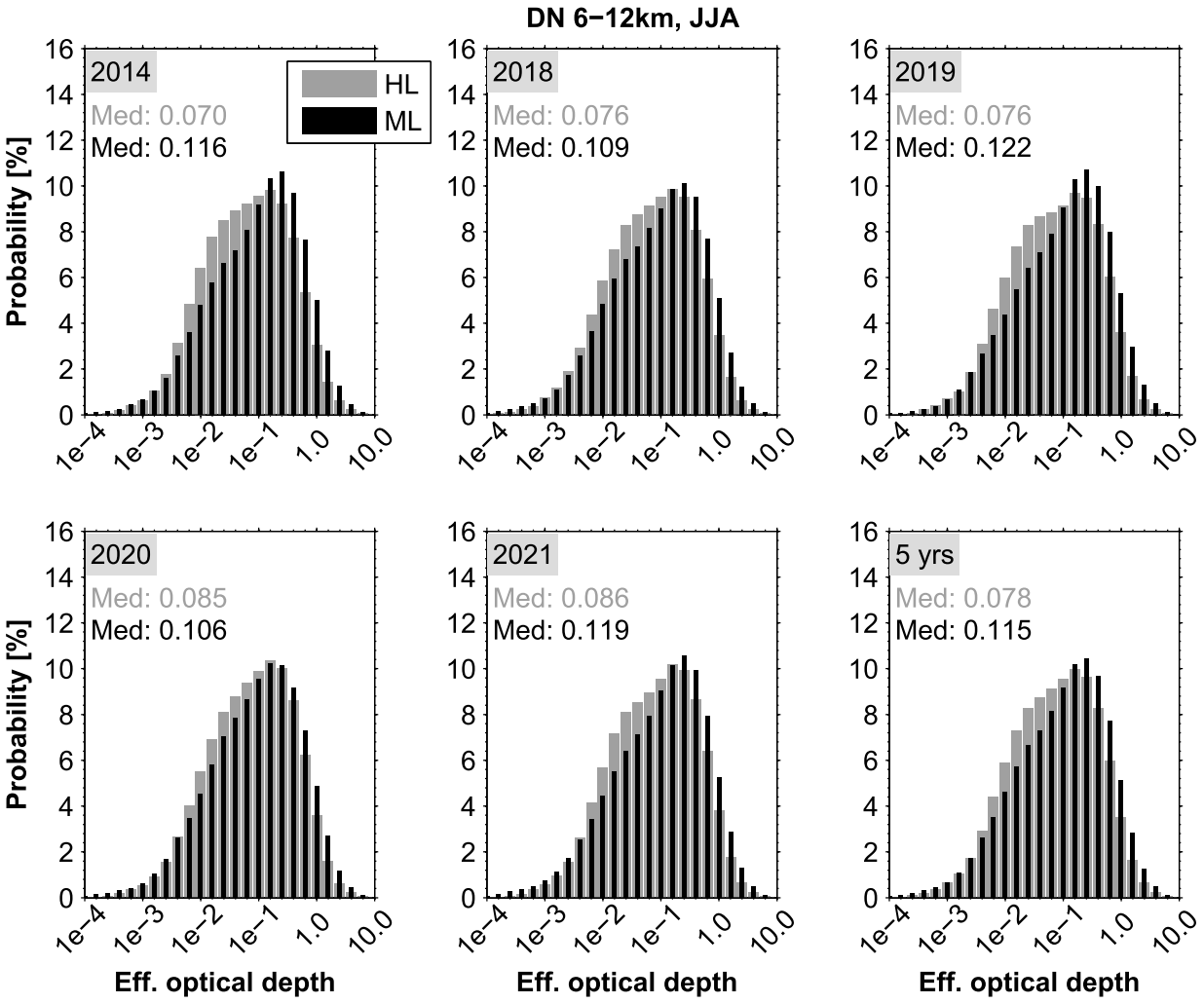

Figure S3. Histograms of effective optical depth of cirrus clouds in summer (JJA: Jun-Jul-Aug) in years of 2014 and 2018–2021 as well as the composite results in the 5 years. The results derived from the measurements at HL and ML are shown in gray and black, respectively.

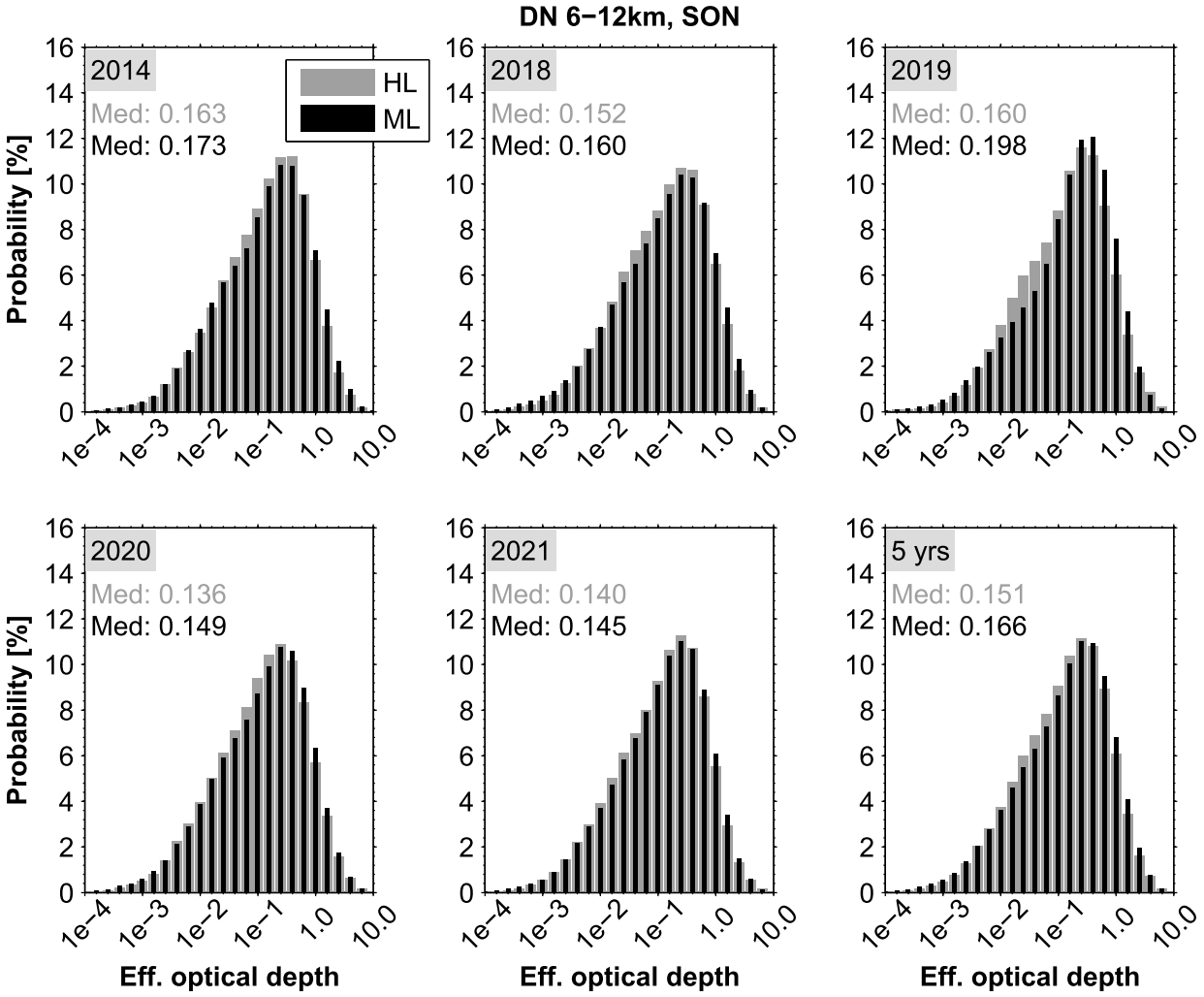

Figure S4. Same as Figure S3, but for autumn (SON: Sep-Oct-Nov).

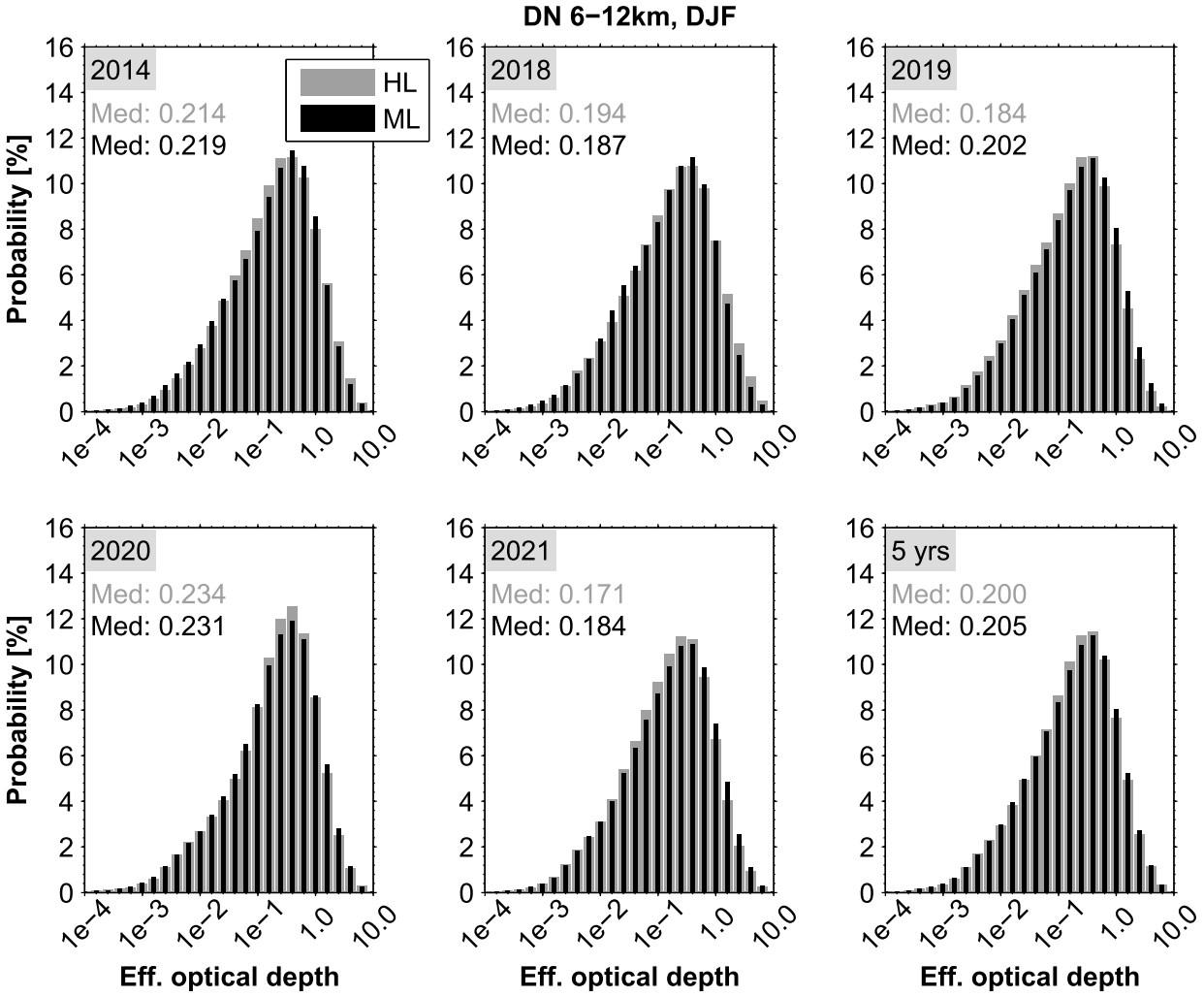

Figure S5. Same as Figure S3, but for winter (DJF: Dec-Jan-Feb).

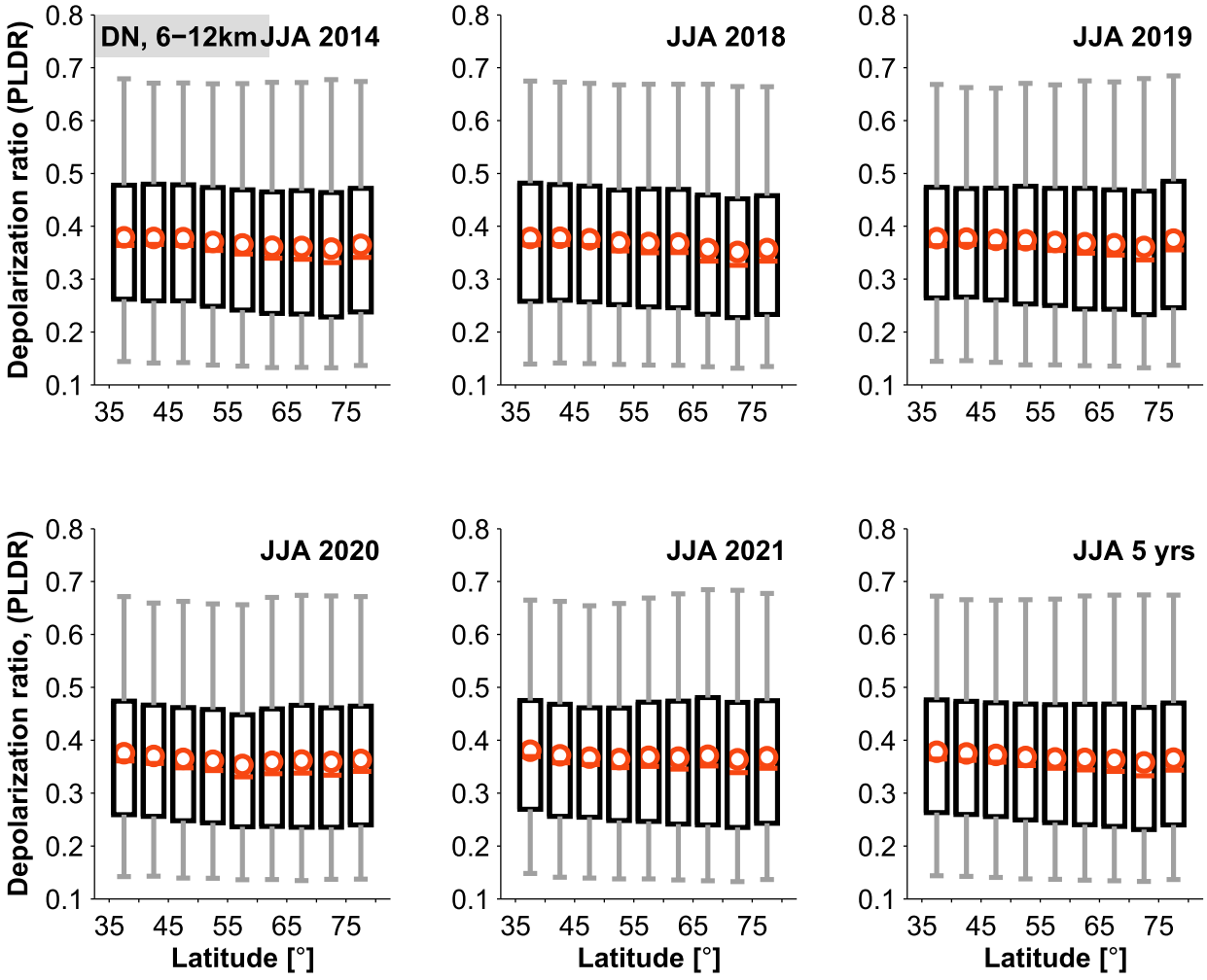

Figure S6. Box plot representations of the composite distributions of particle linear depolarization ratios (PLDR) of cirrus clouds in each 5-degree latitude bin from 35–80°N in summer in years of 2014 and 2018–2021 as well as the composite results of all the 5 years. Boxes represent the 25th–75th percentiles of the PLDR distributions (top and bottom, respectively). Solid lines through the corresponding boxes stand for the medians and circles for the means. Whiskers indicate the 5th and 95th percentiles, and outliers with values falling within the largest 5% and the smallest 5% of the PLDR distributions are not shown here.

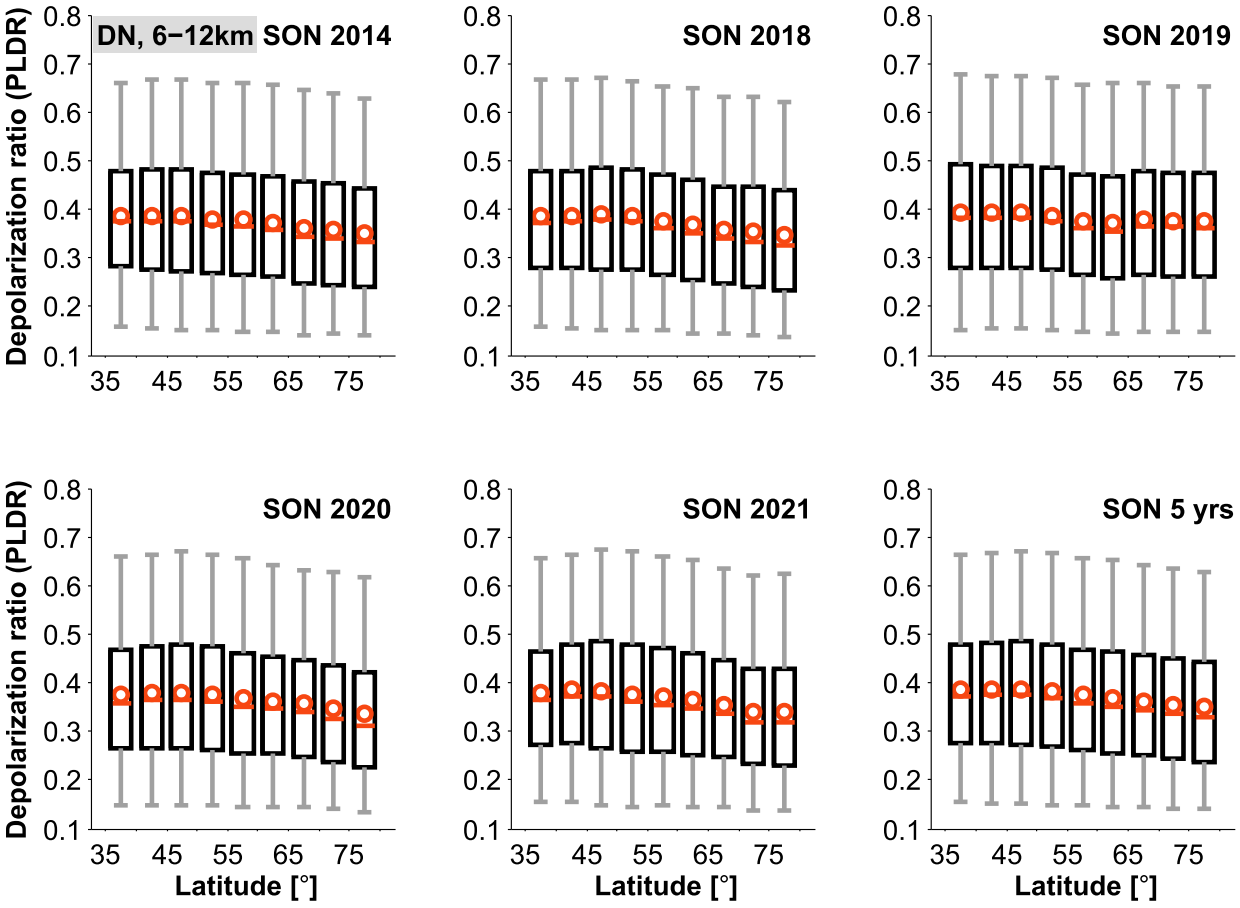

Figure S7. Same as Figure S6, but for autumn.

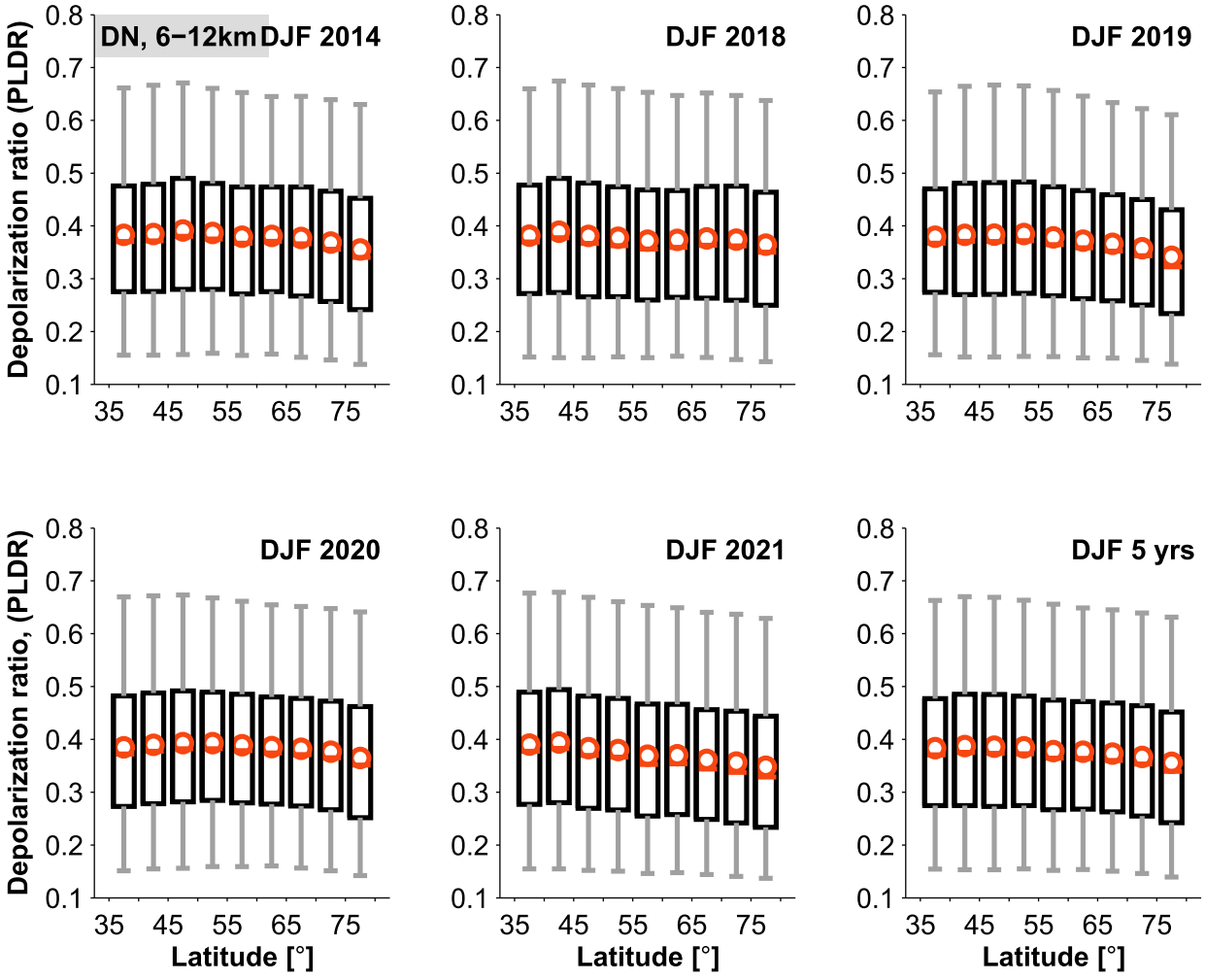

Figure S8. Same as Figure S6, but for winter.

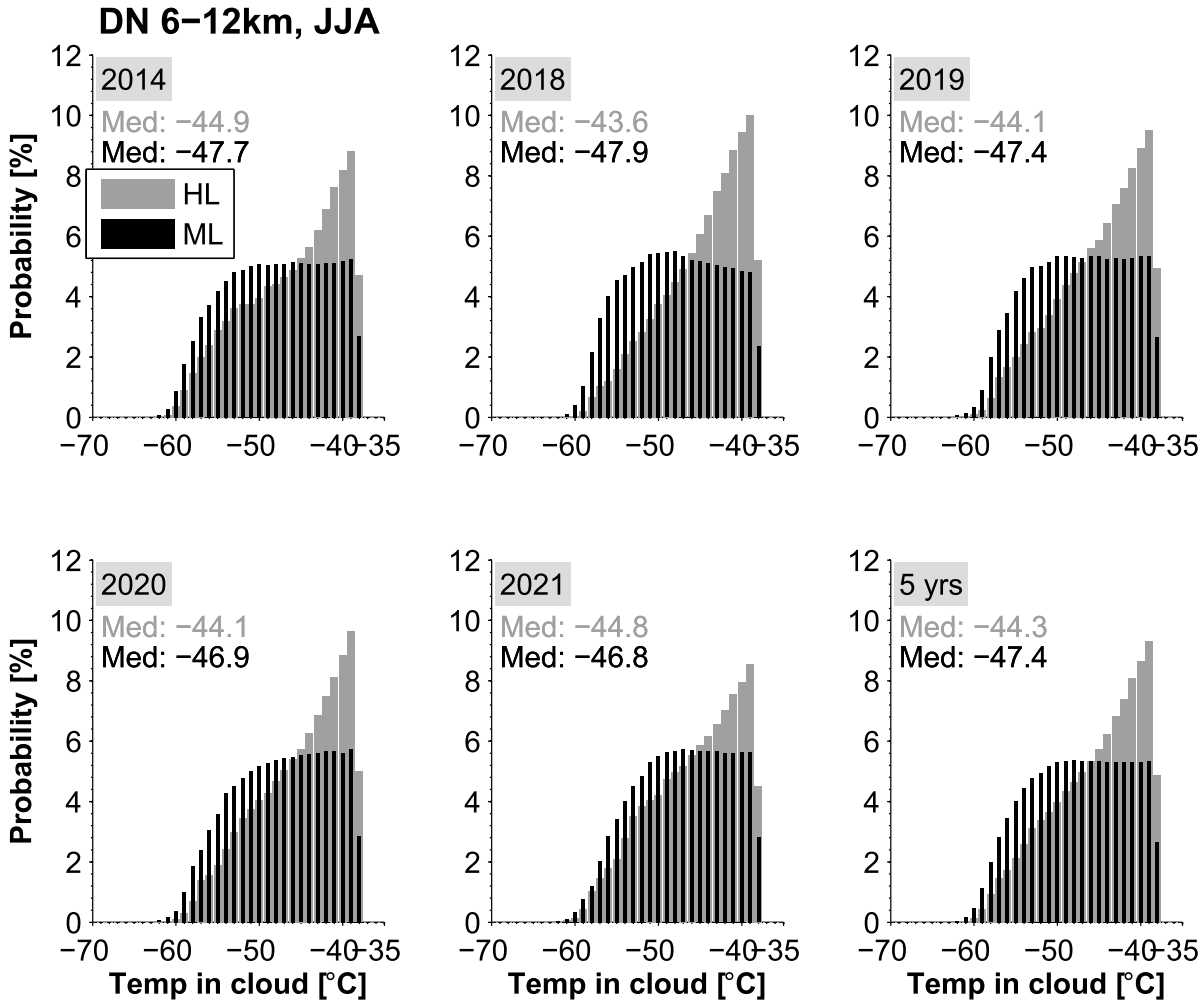

Figure S9. Comparison of temperatures inside cirrus clouds within different latitudes in summer. The histograms at HL are shown in gray and at ML in black with the medians indicated in the insert.

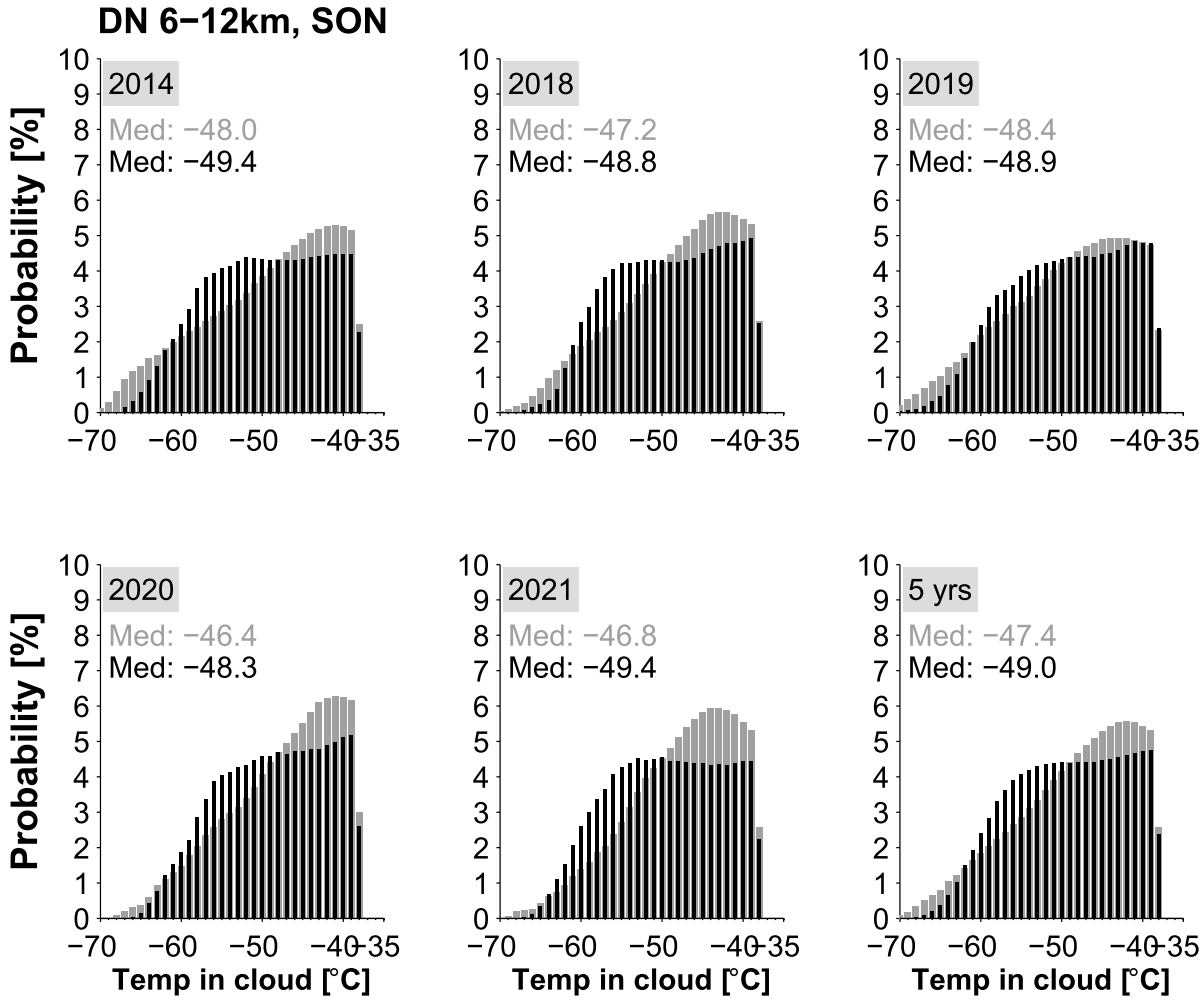

Figure S10. Same as Figure S9, but for autumn.

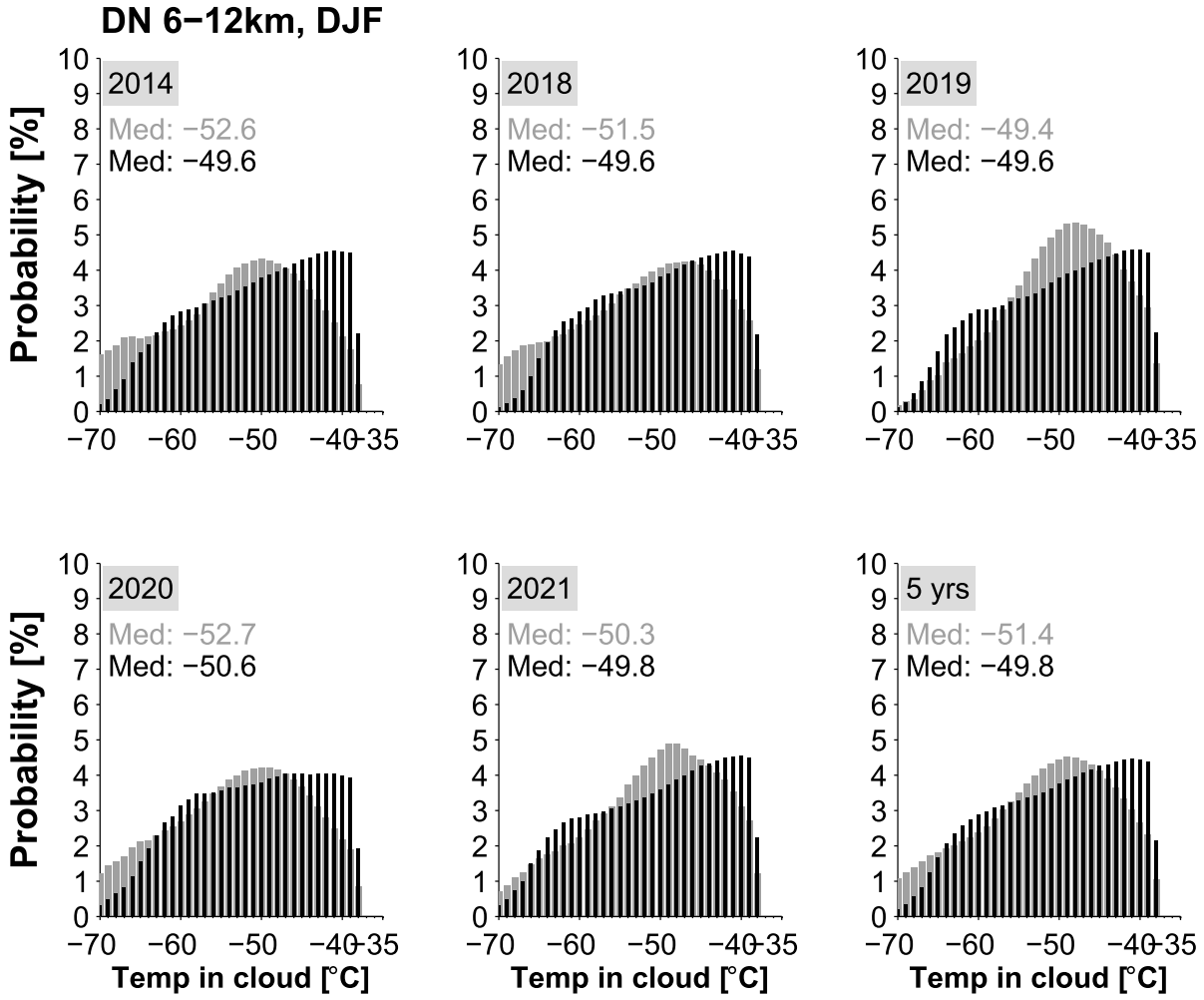

Figure S11. Same as Figure S9, but for winter.